ISBN: 978-3-95450-222-6 ISSN: 2673-5350 doi:10.18429/JACoW-IBIC2020-WEPP10

PROTON-INDUCED SEY FROM BEAM INTERCEPTIVE DEVICES IN THE ESS LINAC

E. M. Donegani*
European Spallation Source ERIC, Lund, Sweden

Abstract

During the ESS linac commissioning, a wealth of beam-interceptive devices will be exposed to protons with nominal and non-nominal energies spanning from 75 keV to 2 GeV. Therefore, a database of proton-induced Secondary Emission Yield (SEY) values was prepared for the structural materials of devices insertable into the ESS linac. The database relies on calculations of collision stopping powers in MCNPX and the Sternglass theory applied to protons in the [0.001, 2000] MeV energy range. Results are reported for relevant materials to wire scanners, bunch shape monitors and target imaging systems: Cu, Ti, Ni, W, SiC, TZM and graphite. In the future, the novel method can be used also for determining the impact of secondaries on emittance or beam-current measurements with Emittance Monitor Units or Faraday cups of the ESS linac, respectively. Moreover, the database can be extended to critical structural materials of the ESS linac itself, in order to estimate the impact of secondary electrons on the overall beam quality.

INTRODUCTION

The European Spallation Source (ESS) in Lund (Sweden) is currently one of the largest science and technology infrastructure projects being built today. The facility will rely on the most powerful linear proton accelerator ever built, a rotating spallation target, 22 state-of-the-art neutron instruments, a suite of laboratories, and a supercomputing data management and software development centre [1]. The ESS accelerator high-level requirements are to provide a 2.86 ms long proton pulse at 2 GeV at repetition rate of 14 Hz. This represents 5 MW of average beam power with a 4% duty cycle on the spallation target [2].

A comprehensive suite of beam instrumentation and diagnostics [3] has started to support the commissioning and operation of the normal-conducting linac (NCL) section of the ESS linac. Additional devices are going to be deployed in the superconducting linac (SCL) section, and finally in the transport lines to the tuning dump and to the spallation target. Therefore, a wealth of beam-interceptive devices will be exposed to protons with nominal and non-nominal energies, spanning from 75 keV to 2 GeV:

- Wire Scanners (WS) [4] and Bunch Shape Monitors (BSM) [3] to determine the transverse and the longitudinal charge distribution, respectively;
- Target imaging systems [5] to detect small fractions of the proton beam that are outside a defined aperture, and to measure the horizontal and vertical beam profiles.

* elena.donegani@ess.eu

The WS, BSM and target imaging systems rely on secondary emission from thin wires or grids, from which a current proportional to the beam intensity is measured. The structural materials of such wires and grids are reported in Table 1.

Table 1: List of beam-interceptive devices in the ESS linac, with the corresponding main structural materials and the proton energy range E_P they are exposed to.

Device	E_P [MeV]	Material
EMU	[0.075, 3.6]	TZM, Cu, W
FC	[0.075, 74]	C, Cu, TZM
BSM	[3.6, 90]	C, W
WS	[3.6, 2000]	C, W
IBS	[73, 360]	Ti
Target imaging	[800, 2000]	Ni, SiC, W

There is another set of beam-interceptive devices whose performance can be severely limited by secondary electrons:

- Faraday cups (FC) [6] whose ability to measure the beam current depends on the capability of recapturing the ejected electrons;
- Emittance Monitor Units (EMU) for measuring the emittance, which can rely either on an internal FC [7] or on slit and grid combination [8];
- Insertable Beam Stops (IBS) [9] which is used to safely stop the beam in a particle-free vacuum environment.

Therefore, a database of SEY values was developed for all the structural materials relevant to the beam-interceptive devices in the ESS linac. The newly developed method for calculating Secondary Emission Yields (SEY), induced by protons in the [0.001, 2000] MeV range, is described in the following paragraph.

METHOD

The novel method for calculating the SEY is based on quick calculations of stopping powers in MCNPX [10] and the Sternglass theory [11]. As a first step, a cylindrical rod of the material of interest is simulated in MCNPX; the radius is set equal to two Molière radius, while the length is set long enough to fully contain a beam of 2 GeV protons.

The proton beam is defined as a monoenergetic source of 2 GeV protons, with a Gaussian distribution having σ=0.6 cm. The beam is perpendicularly impinging on the base of the cylindrical rod. In addition to protons, also electrons, neutrons and photons are transported. One single run

ISBN: 978-3-95450-222-6 ISSN: 2673-5350 doi:10.18429/JACoW-IBIC2020-WEPP10

with 1E5 proton histories takes approximately 10 minutes on a standard laptop and provides the collision, radiation and total stopping powers for protons from 2 GeV down to 1 keV. Since in proton-induced SEY calculations it is important to compute the amount of energy lost by protons, the collision stopping power dE/dx is considered (in MeV·cm^2/g).

As a second step, the number of electrons per primary proton (i.e. the SEY) is computed according to the Sternglass formula:

$$SEY = \frac{P \cdot \rho \cdot t}{25\ eV} \cdot \frac{dE}{dx}, \qquad (1)$$

where $P = 0.5$ is the probability that an electron escapes from the material surface, ρ is the material density (in g/cm^3) and t is the mean free path of secondary electrons which is set equal to 1 nm. Since the average energy of the secondary electrons is estimated to be in the 20 eV-30 eV range by Sternglass [11], the value of 25 eV appears at the denominator of Eq. (1). The SEY values calculated for the materials and compounds of current interest are summarized in the following paragraph.

RESULTS

The presented method was validated with four elements for which dE/dx values were available from NIST [12]: Al, Cu, Fe and W. The novel method was therefore applied also to all the materials and compounds previously listed in Table 1. As representative example, the calculated SEY values are plotted in Fig. 1 in the case of nickel, for which no data were found available from NIST throughout the proton energy range of interest for the present work.

As expected from Eq. (1), the SEY curve in Fig. 1 follows the trend of the dE/dx distribution, spanning over three orders of magnitude for proton energies in the [0.001, 2000] MeV range. A peak is usually observed around 100 keV, then the SEY values monotonically decrease for increasing proton energies up to 2 GeV. This is an important aspect to be considered for insertable devices in the NCL linac, where the SEY is maximal. The SEY values at relevant energies in the ESS NCL are reported in Table 2. The maximum SEY value is found after 75 keV protons on TZM - a molybdenum alloy which is used in the LEBT EMU and in the energy degrader of a DTL FC.

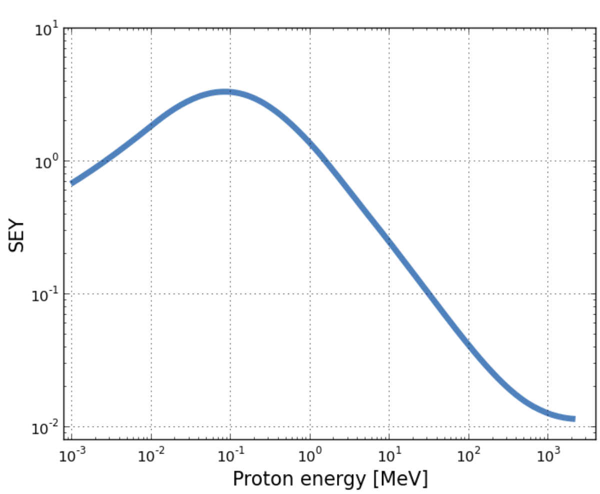

Figure 1: Calculated SEY values by protons in nickel.

The SEY values at relevant energies in the ESS SCL are reported in Table 3. The energies of 800 MeV and 2 GeV are the initial and final intended energy of the beam on target, respectively. At the highest energy considered, the maximum SEY values is found for protons on tungsten.

Any other SEY value at any non-nominal beam energy can be easily inferred from the available dataset.

Table 2: Calculated SEY values for relevant proton energies and structural materials of beam-interceptive devices in the ESS NCL section.

E_P [MeV]	**0.075**	**3.6**	**21**	**74**
C	2.238	0.315	0.080	0.029
Ti	2.527	0.551	0.152	0.058
Ni	2.695	1.033	0.293	0.113
Cu	2.560	0.982	0.280	0.108
W	2.971	1.339	0.432	0.175
TZM	3.400	0.960	0.285	0.113
SiC	1.604	0.537	0.137	0.050

Table 3: Calculated SEY values for relevant proton energies and structural materials of beam-interceptive devices in the ESS SCL section.

E_P[MeV]	**90**	**360**	**800**	**2000**
C	0.025	0.010	0.008	0.006
Ti	0.050	0.021	0.015	0.013
Ni	0.098	0.041	0.030	0.027
Cu	0.094	0.039	0.029	0.026
W	0.154	0.067	0.050	0.045
TZM	0.098	0.042	0.031	0.028
SiC	0.044	0.018	0.013	0.011

CONCLUSIONS AND OUTLOOK

The method for calculating SEY values in key structural materials of the devices insertable into the ESS linac was presented. The results are based on fast yet reliable MCNPX calculations and on the Sternglass theory. Proton-induced SEY values were calculated over six orders of magnitude i.e. from 1 keV up to 2 GeV. The lookup tables serve for beam-current estimations, both at nominal and non-nominal beam energies during the ESS linac commissioning. The possibilities offered by the newly developed method are manifold. Since it's virtually possible to define in MCNPX any density, isotope and chemical composition, the method is useful for selecting novel materials and compounds which may be needed for detectors upgrades. Moreover, it enables to explore the impact of oxides on metallic surfaces. In addition, the presented method can help in investigating the

ISBN: 978-3-95450-222-6 ISSN: 2673-5350 doi:10.18429/JACoW-IBIC2020-WEPP10

impact of secondaries on key linac components that could be affected by e.g. the multipacting effect. In the future, it would be useful to further develop the presented method to account for temperature and radiation-induced effects on SEY.

ACKNOWLEDGMENTS

The author is grateful to Dr. Cyrille Thomas and the colleagues working on the ESS target imaging system for having triggered the work presented in this paper. In fact, the presented method was initially developed just for the key materials of the aperture monitor and grid system for the beam on the ESS target, recognized to be universally useful and thus applied to the structural materials of all the other beam-interceptive devices in the ESS linac.

REFERENCES

[1] ESS, https://europeanspallationsource.se/about

[2] R. Garoby *et al.*, "Corrigendum: the European Spallation Source design", *Phys. Scr.*, vol. 93, p. 014001, 2018. doi:10.1088/1402-4896/aaecea

[3] T. J. Shea *et al.*, "Overview and status of diagnostics for the ESS project", in *Proc. 6th Int. Beam Instrumentation Conf. (IBIC'17)*, Grand Rapids, MI, USA, Aug. 2017, pp. 8–15. doi:10.18429/JACoW-IBIC2017-MO2AB2

[4] S. Grulja, S. Cleva, R. De Monte, and M. Ferianis, "Wire scanner diagnostic system", in *Proc. 8th Int. Beam Instrumentation Conf. (IBIC'19)*, Malmö, Sweden, Sep. 2019, pp. 326–327. doi:10.18429/JACoW-IBIC2019-TUPP015

[5] C. A. Thomas *et al.*, "J-PARC test of ESS beam on target diagnostics prototypes aperture monitor and GRID", in *Proc. 8th Int. Beam Instrumentation Conf. (IBIC'19)*, Malmö, Sweden, Sep. 2019, pp. 387–391. doi:10.18429/JACoW-IBIC2019-TUPP032

[6] E. M. Donegani, I. Bustinduy, C. S. Derrez, T. J. Grandsaert, A. Rodríguez Páramo, and T. J. Shea, "Status of the Faraday Cups for the ESS Linac", in *Proc. 8th Int. Beam Instrumentation Conf. (IBIC'19)*, Malmö, Sweden, Sep. 2019, pp. 205–208. doi:10.18429/JACoW-IBIC2019-MOPP044

[7] O. Tuske *et al.*, "ESS emittance measurements at INFN CATANIA", in *Proc. 8th Int. Particle Accelerator Conf. (IPAC'17)*, Copenhagen, Denmark, May 2017, pp. 123–125. doi:10.18429/JACoW-IPAC2017-MOPAB023

[8] B. Cheymol and A. Ponton, "High power and high duty cycle slit and grid system for hadron accelerator commissioning", in *Proc. 57th ICFA Advanced Beam Dynamics Workshop on High-Intensity and High-Brightness Hadron Beams (HB'16)*, Malmö, Sweden, Jul. 2016, pp. 226–231. doi:10.18429/JACoW-HB2016-MOPL017

[9] E. M. Donegani, T. J. Grandsaert, T. J. Shea, and C. A. Thomas, "The insertable beam stop in the ESS SPK section", presented at the 9th Int. Beam Instrumentation Conf. (IBIC'20), Santos, Brazil, Sep. 2020, paper WEPP07, this conference.

[10] D. B. Pelowitz, Ed., "MCNPX Users Manual Version 2.7.0", LA-CP-11-00438, 2011.

[11] E. J. Sternglass, "Theory of secondary electron emission by high-speed ions", *Phys. Rev.*, vol. 108, p. 1, 1957. doi:10.1103/PhysRev.108.1

[12] "Stopping-Power and Range Tables for Electrons, Protons, and Helium Ions", NIST Standard Reference Database 124, https://physics.nist.gov/PhysRefData/Star/Text/PSTAR.html